

## INFLUENCE OF PRECURSOR TYPE AND CONCENTRATION ON THE SYNTHESIS OF COPPER SULFIDE NANOPARTICLES

O. O. BALAYEVA<sup>a\*</sup>, A. A. AZIZOV<sup>a</sup>, M. B. MURADOV<sup>b</sup>,  
G. M. EYVAZOVA<sup>b</sup>, R. M. ALOSMAOV<sup>a</sup>

<sup>a</sup> *Department of Chemistry, Baku State University, Z. Khalilov str., 23, AZ-1148 Baku, Azerbaijan*

<sup>b</sup> *Department of Physics, Baku State University, Z. Khalilov str., 23, AZ-1148 Baku, Azerbaijan*

Copper sulfide nanoparticles were successfully synthesized on the base of functionalized nitrile butadiene rubber (FNBR) at room temperature by the successive ionic layer adsorption and reaction (SILAR) method using  $\text{CuSO}_4 \times 5\text{H}_2\text{O}$ ,  $\text{CuCl}_2 \times 2\text{H}_2\text{O}$  aqueous solutions as a copper precursors;  $\text{Na}_2\text{S} \times 9\text{H}_2\text{O}$  and thiourea  $[(\text{NH}_2)_2\text{CS}]$  aqueous solutions as sulfur precursors. X-ray diffractometer (XRD), scanning electron microscopy (SEM), energy-dispersive X-ray spectrometer (EDX), ultraviolet–visible (UV–Vis) and Fourier transform infrared (FTIR) spectrometer were used to characterize the products. Obtained copper sulfide nanocomposites were heated at 100°C temperature in a vacuum.

(Received November 7, 2016; January 20, 2017)

*Keywords:* copper sulfide, FNBR, nanocomposites, optical and structural properties

### 1. Introduction

$\text{Cu}_x\text{S}$  are the significant binary compounds synthesized on a large scale with controlled morphology, size, composition, and structure lie at the heart of their practical applications. They are well known to form a wide variety of non-stoichiometric and mixed phases, of which at least five species are known to be stable at room temperature: covellite ( $\text{CuS}$ ) in the sulfur-rich region, and annilite ( $\text{Cu}_{1.75}\text{S}$ ), digenite ( $\text{Cu}_{1.8}\text{S}$ ), djurleite ( $\text{Cu}_{1.95}\text{S}$ ) and Chalcocite ( $\text{Cu}_2\text{S}$ ) in the copper-rich region [1]. Nanostructured copper sulfide grows with 0-D (quantum dots [2], 1-D (nanotubes [3]; nanowires [3,4]; nanorods [5,6]; nanoneedles [7]), 2-D (nanoplates [8]; nanoribbons [9]; nanodisks [10]; nanosheets [7,11,12]) and 3-D (nanocubes [13], nanospheres [14-16], cages [17]) using different synthesis methods exhibit size and shape dependent properties and have potential applications in various fields, such as materials science; biomedical science; electronics; optics; energy storage, electrochemistry and so on.

Using  $\text{CuSO}_4 \times 5\text{H}_2\text{O}$  and  $\text{Cu}(\text{NO}_3)_2$  as a copper precursor, nanocrystalline copper sulfide with different phases like  $\text{Cu}_7\text{S}_4$  [17],  $\text{Cu}_2\text{S}$  [18-20],  $\text{CuS}$  [12,21],  $\text{Cu}_{1.81}\text{S}$  [22,23],  $\text{Cu}_{1.97}\text{S}$  [2] have been obtained.

The band gap of these  $\text{Cu}_{2-x}\text{S}$  exhibits stoichiometry dependence. An increase in the band gap occurs with an increase of the “x” value in bulk copper sulfides ( $E_g$ ) 1.2 eV for  $\text{Cu}_2\text{S}$ , 1.5 eV for  $\text{Cu}_{1.8}\text{S}$  and 2.0 eV for  $\text{CuS}$  [24-26]. Generally, SILAR method includes the mononuclear growth and by this method, we can control the size of nanoparticles carefully. The size or thickness of the nanoparticles is usually controlled by the number of deposition cycles.

Herein, we propose a simple successive ionic layer adsorption and reaction (SILAR) process for the synthesis of copper sulfide nanoparticles with  $\text{CuCl}_2 \times 2\text{H}_2\text{O}$ ,  $\text{CuSO}_4 \times 5\text{H}_2\text{O}$ , and thiourea as the reactants at room temperature. The aim of this study is to establish the optical properties (Absorbance, Transmittance and Band gap), structural properties (phase and structure) of copper sulfide nanoparticles and the influence of precursor type, concentration, reaction parameters were studied.

---

\* Corresponding author: ofeliya1989@inbox.ru

## 2. Experimental

### 2.1. Materials and instrumentation

All chemicals (synthetically nitrile butadiene rubber (NBR-26), phosphorus trichloride ( $\text{PCl}_3$ ),  $\text{CuSO}_4 \times 5\text{H}_2\text{O}$ ,  $\text{CuCl}_2 \times 2\text{H}_2\text{O}$ ,  $\text{Na}_2\text{S} \times 9\text{H}_2\text{O}$ ,  $\text{S}=\text{C}(\text{NH}_2)_2$ , and  $\text{KOH}$ ) were used for the preparation of  $\text{Cu}_x\text{S}_y/\text{FNBR}$  nanocomposites were of analytical grade.

XRD patterns of the samples were recorded by using of Bruker D2 Phaser Advance X-ray diffractometer with  $\text{Cu K}\alpha$  irradiation ( $\lambda = 1.54060 \text{ \AA}$ ), UV-Vis absorption spectra and FTIR spectra were reflected whereby SPECORD 250 PLUS and VARIAN 3600, respectively. SEM/EDX analysis was carried out on a Field Emission Scanning Electron Microscope JEOL JSM-7600F with Energy dispersive spectrometer X-max 50.

### 2.2. Synthesis of $\text{CuS}/\text{FNBR}$ and $\text{Cu}_{1.8}\text{S}/\text{FNBR}$ nanocomposites using $\text{Na}_2\text{S}$ as sulfur source and different type of copper precursor

Functionalized nitrile butadiene rubber (FNBR) containing  $-\text{PO}(\text{OH})_2$  and  $-\text{OPO}(\text{OH})_2$  functional active groups were synthesized from the oxidative chlorophosphonation reaction of NBR with  $\text{PCl}_3$  and oxygen [27-29]. The phosphorus-containing polymer sorbent (FNBR) is dark brown powder. The preparation of copper sulfide nanoparticles was carried out by a successive ionic layer adsorption and reaction (SILAR) method. Two solutions of 25 ml 0.5 M  $\text{CuCl}_2 \times 2\text{H}_2\text{O}$  and 25ml 0.1 M  $\text{CuSO}_4 \times 5\text{H}_2\text{O}$  were prepared as copper precursors. 0.2 g of FNBR powders were added to every solution at room temperature. After 24 hours, polymers containing  $\text{Cu}^{2+}$  ions were washed with distilled water. In the sulfurizing processes 25 ml 0.1M of  $\text{Na}_2\text{S} \times 9\text{H}_2\text{O}$  were added and stirred for 24 hours for Sample B, and 3 hours for Sample A. Samples were washed with distilled water and air-dried. The formation were carried out and in 6 and 8 cycles.

Table 1. Copper sulfide nanostructures deposited on FNBR at different preparation conditions.

Samples	Comp.	Concent. of $\text{Cu}^{2+}$ (M)	"S" sources	Concent. of $\text{S}^{2-}$ (M)	"Cu" sources	Immersion time of $\text{Ni}^{2+}$ ions	Sulfurizing time
Sample A	$\text{Cu}_{1.8}\text{S}$	0.1	$\text{Na}_2\text{S}$	0.1	$\text{CuSO}_4 \times 5\text{H}_2\text{O}$	24 h	3 h
Sample B	$\text{CuS}$	0.5	$\text{Na}_2\text{S}$	0.1	$\text{CuCl}_2 \times 2\text{H}_2\text{O}$	24 h	24 h
Sample C	$\text{CuS}$	0.5	Thiourea	1	$\text{CuCl}_2 \times 2\text{H}_2\text{O}$	24 h	24 h

### 2.3. Synthesis of $\text{CuS}/\text{FNBR}$ nanocomposite using thiourea as a sulfur source

In a typical preparation 25 ml 0.5 M  $\text{CuCl}_2 \times 2\text{H}_2\text{O}$  water solution was prepared as a copper precursor for the synthesis of  $\text{CuS}$  nanoparticles shown in Table 1 (Sample C). 0.2 g of FNBR powders were added to this solution at room temperature. After 24 hours, polymers containing  $\text{Cu}^{2+}$  ions were washed to remove unexchanged ions. The sulfurizing processes were carried out with 25 ml 1M of thiourea, stirred for 24h and washed with distilled water. Then 25 ml 1M of  $\text{KOH}$  solution was added to this sample and stirred 24 hours. The sample was rinsed up with distilled water and this process was repeated in 6 and 8 cycles and air-dried. All samples were heated at  $100 \text{ }^\circ\text{C}$  temperature in a vacuum. The nucleation processes occur in the first cycle and then the process goes with the formation of copper sulfide nanoparticles [29].



or





### 3. Results and discussions

#### 3.1. Structural properties by XRD

The structural properties of the copper sulfide samples ( $\text{Cu}_x\text{S}_y$ ) depends on the synthesis process and the reaction medium. To know the crystalline phase of the deposited copper sulfide, XRD analysis was carried out (Fig. 1).

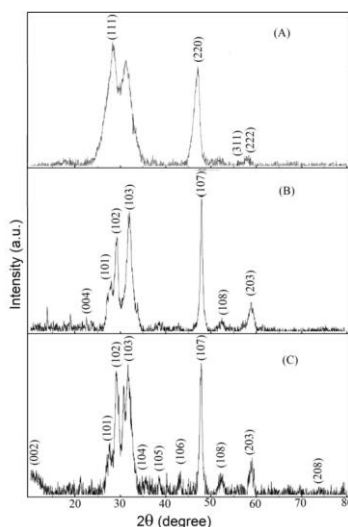


Fig. 1. XRD patterns of (A)  $\text{Cu}_{1.8}\text{S}/\text{FNBR}$  prepared in 3h sulfurizing time using 0.1M  $\text{Na}_2\text{S}$  and 0.1M  $\text{CuSO}_4 \times 5\text{H}_2\text{O}$  as precursors, (B)  $\text{CuS}/\text{FNBR}$  prepared in 24h sulfurizing time using 0.1M  $\text{Na}_2\text{S}$  and 0.5M  $\text{CuCl}_2 \times 2\text{H}_2\text{O}$  as precursors. (C)  $\text{CuS}/\text{FNBR}$  prepared in 24h sulfurizing time using 1M thiourea and 0.5M  $\text{CuCl}_2 \times 2\text{H}_2\text{O}$  as precursors.

There are basically three high intensity diffraction peaks at  $2\theta = 28^\circ, 33^\circ, 47^\circ$  from the (111), (200), (220) planes, respectively for Sample A,  $2\theta = 29.5^\circ, 31.7^\circ, 47.5^\circ$  from the (102), (103), (107) planes, respectively for Sample B and Sample C whereas, a very small diffraction peak from (222) plane was obtained at  $2\theta = 58.5^\circ$  for Sample A, and lots of small diffraction peaks from (101), (104), (105), (106), (108), (203), (208) planes were obtained at  $2\theta = 27.5^\circ, 35.5^\circ, 38^\circ, 42.7^\circ, 52.7^\circ, 58.8^\circ$  for Sample B and C. This indicates that the obtained  $\text{CuS}$  were nanocrystalline in nature. From the XRD pattern, no other characteristic peaks corresponding to any impurity was obtained, indicating the purity of the product (JCPDS Card No.00-006-0464) (Fig. 2). The XRD pattern of Sample A using  $\text{CuSO}_4 \times 5\text{H}_2\text{O}$  was shown in Fig. 1A. All peaks could be indexed as cubic  $\text{Cu}_{1.8}\text{S}$ . The calculated cell constant  $a=5.9315\text{\AA}$ , which is consistent with the reported values (JCPDS Card No. 24-0061). No characteristic peaks of other impurities were observed. Using  $\text{CuCl}_2 \times 2\text{H}_2\text{O}$  as a copper precursor in different sulfur sources like sodium sulfide and thiourea, phase-pure hexagonal  $\text{CuS}$  nanocrystals were synthesized (Fig. 1B,C). The formation of different crystal phases like  $\text{Cu}_{1.8}\text{S}$  and  $\text{CuS}$  can be explained as due to the copper precursors.  $\text{CuSO}_4 \times 5\text{H}_2\text{O}$  has an oxidizing nature and by this precursor, the reaction goes by the formation of not II valence copper sulfide. But the reaction with  $\text{CuCl}_2 \times 2\text{H}_2\text{O}$  goes by the formation of pure hexagonal covellite  $\text{CuS}$ . In this way, the synthesis of II valence copper sulfide can be explained that the ion exchange reaction occurred in the process. The average particle size of  $\text{CuS}$  and  $\text{Cu}_{1.8}\text{S}$  were in the range of 10-10.8 nm and 5-7 nm by XRD, respectively.

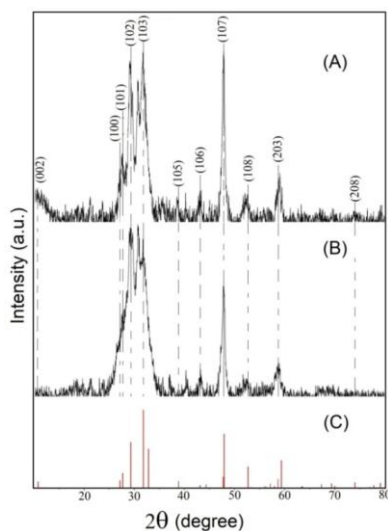


Fig. 2. XRD patterns of CuS/FNBR prepared in 24h sulfuring time using 1M of thiourea and 0.5M  $\text{CuCl}_2 \cdot 2\text{H}_2\text{O}$  as precursors. A) 8 cycles; B) 6 cycles; C) JCPDS Card No.00-006-0464 of CuS.

### 3.2. Optical properties

The optical transmittance of CuS/FNBR nanocomposites in different reaction parameters and temperature were investigated in the 300–800 nm wavelength range by UV-Vis spectroscopy (Fig. 3A). The recorded data was further used to calculate the band gap energy of the CuS nanoparticles.

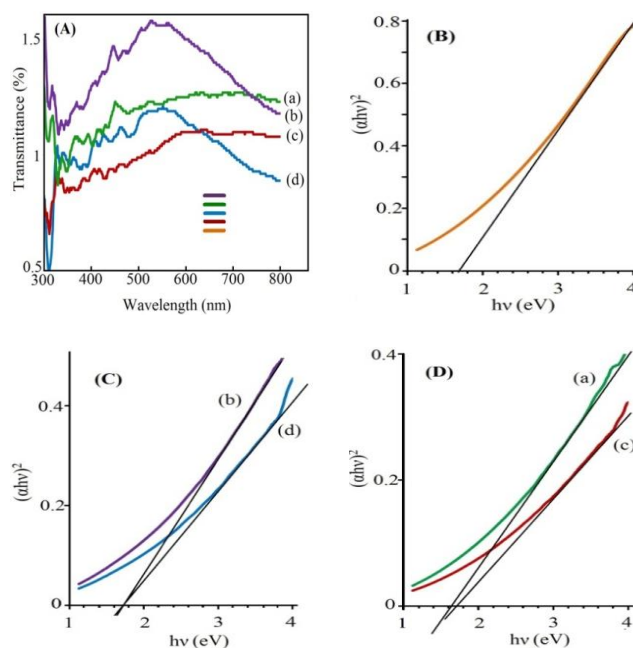


Fig. 3. Optical transmittance plot of CuS prepared using (a) thiourea as a sulfur precursor and heated 100°C, (b)  $\text{Na}_2\text{S}$  as a sulfur precursor and heated 100 °C, (c) thiourea as sulfur precursor, (d)  $\text{Na}_2\text{S}$  as a sulfur precursor (A). Corresponding bandgap plots of  $\text{Cu}_{1.8}\text{S}$  (B) and CuS (C) and (D) prepared using (a) thiourea as a sulfur precursor and heated 100°C, (b)  $\text{Na}_2\text{S}$  as a sulfur precursor and heated 100 °C, (c) thiourea as sulfur precursor, (d)  $\text{Na}_2\text{S}$  as a sulfur precursor.

Fig. 3(B,C,D) shows the plot of  $(\alpha h\nu)^2$  versus  $h\nu$ , which is a straight line in the domain of higher energies, indicating a direct optical transition. The band gap energy is obtained by extrapolating the linear portion of  $(\alpha h\nu)^2$  versus  $h\nu$  plot to the energy axis. The observed direct band gap energy is 1.68 eV for  $\text{Cu}_{1.8}\text{S}$  obtained in 3h sulfurizing time using 0.1M  $\text{Na}_2\text{S}$  and 0.1M  $\text{CuSO}_4 \times 5\text{H}_2\text{O}$  as precursors. The band gap of  $\text{Cu}_{2-x}\text{S}$  exhibits stoichiometry dependence. An increase in the band gap occurs with an increase of the x value in bulk copper sulfides ( $E_g$ ) 1.2 eV for  $\text{Cu}_2\text{S}$ , 1.5 eV for  $\text{Cu}_{1.8}\text{S}$  and 2 eV for  $\text{CuS}$  [24-26]. The band gaps for  $\text{CuS}$  nanoparticles obtained different sulfur sources like  $\text{Na}_2\text{S}$  and thiourea were determined to be 1.7 eV and 1.72 eV, respectively. The absorption spectra show a blue shift compared to that of the bulk  $\text{CuS}$ . Normally, the room temperature band gap energy for the bulk  $\text{CuS}$  system is about 2 eV. But the polymer nature and temperature are also the influence of the optical band gap value. In their work Joyjit Kundu and Debabrata Pradhan [30] found that the measured band gap is 1.75 eV for  $\text{CuS}$  prepared at 150 °C whereas it is 1.68 eV for  $\text{CuS}$  prepared at 180 °C and 250 °C. After heating the samples to 100 °C the optical band gap didn't change for  $\text{CuS}$  using  $\text{Na}_2\text{S}$  as a sulfur source and decreased from 1.72 eV to 1.63eV for  $\text{CuS}$  obtained using thiourea Fig. 3C,D). This is due to coalescing of smaller crystallites to form larger particles to low Gibb's free energy by the heating of samples [31].

### 3.3. SEM and EDX analysis

The control at the nanoscale of the composition and morphology of copper chalcogenides is an especially interesting case, because of their stoichiometry-dependent properties and applications [32].

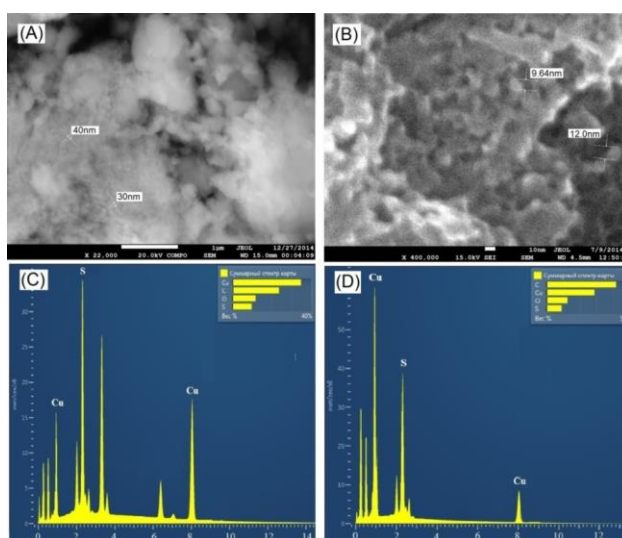


Fig. 4. SEM (A,B) and EDX (C,D) results of  $\text{CuS}/\text{FNBR}$  (A,C) and  $\text{Cu}_{1.8}\text{S}/\text{FNBR}$  (B,D)

Spherical digenite and covellite were obtained in this experiment. Fig. 4A,B exhibits SEM images of as-prepared  $\text{CuS}/\text{FNBR}$  and  $\text{Cu}_{1.8}\text{S}/\text{FNBR}$  nanocomposites obtained using different copper and sulfur precursors. The average particle size of  $\text{CuS}$  and  $\text{Cu}_{1.8}\text{S}$  were determined from the figure is in the range of 30-40 nm and 9-12 nm, respectively which is slightly higher than the value obtained from XRD analysis. This is due to coalescing of smaller crystallites to form larger particles to lower Gibb's free energy. The structure was found to be compact and covered by the polymer material surface.

Samples were analyzed and studied the elemental composition of the phases (Fig 4C,D). Energy dispersive X-ray analysis of copper sulfide was performed using energy dispersive spectrometer. The element ratio of  $\text{Cu}:\text{S}$  was found to be 4:3.8 and 2:1 for  $\text{CuS}$  and  $\text{Cu}_{1.8}\text{S}$  nanoparticles. To confirm the elemental composition of the phase was carried out mapping of the distribution of elements on the surface (Fig. 5).

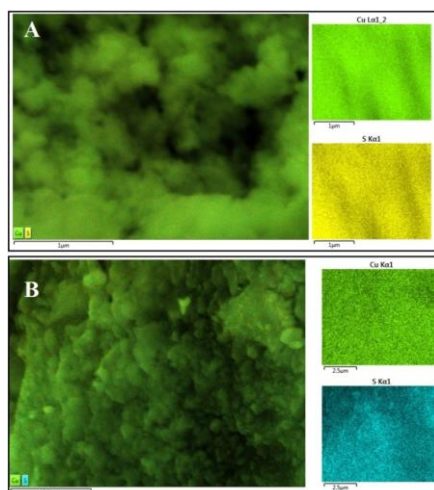


Fig. 5. Mapping images of CuS/FNBR (A) and Cu<sub>1.8</sub>S/FNBR (B) nanocomposites.

### 3.4. FTIR spectroscopy study

The FTIR spectroscopy of the FNBR, CuS/FNBR, and Cu<sub>1.8</sub>S/FNBR obtained using different precursors has been done after and before heating in a vacuum (Fig. 6). The broadband at 2100 cm<sup>-1</sup> and 2191 cm<sup>-1</sup> can be assigned as the O–H stretching peak of the –OPO(OH)<sub>2</sub> group formed by the chlorophosphonation reaction of the polymer. Upon the formation of copper sulfide nanoparticles in all samples, these peaks have been disappearing. The typical bands of polymer sorbent like OH (H<sub>2</sub>O) [33,34]: 3429, C–H: 2920 cm<sup>-1</sup>, O–H (P–O–H): 2854 cm<sup>-1</sup>, O–H [–OPO(OH)<sub>2</sub>]: 2100 cm<sup>-1</sup> and 2191 cm<sup>-1</sup>, P=O (resonance state): 1652 cm<sup>-1</sup> and C–O (P–C–O): 1009 cm<sup>-1</sup> are assigned in the FTIR spectrum. The peak of PO<sub>3</sub><sup>2-</sup> at 977 cm<sup>-1</sup> (Fig. 6e) shift to 941 cm<sup>-1</sup> (Fig. 6a) and 945 cm<sup>-1</sup> (Fig. 6c) upon the formation of Cu<sub>1.8</sub>S and CuS nanoparticles, respectively. Three new bands at about 617 cm<sup>-1</sup>, 611 cm<sup>-1</sup> and 609 cm<sup>-1</sup> are also seen in the copper sulfides/FNBR spectra can be attributed to the Cu–S vibration modes in copper sulfide [35]. The weak band at 1377 cm<sup>-1</sup> assigned as Cu(S=C(NH<sub>2</sub>)<sub>2</sub>)<sub>3</sub>Cl (Fig 6c ) obtained using thiourea as a sulfur precursor.

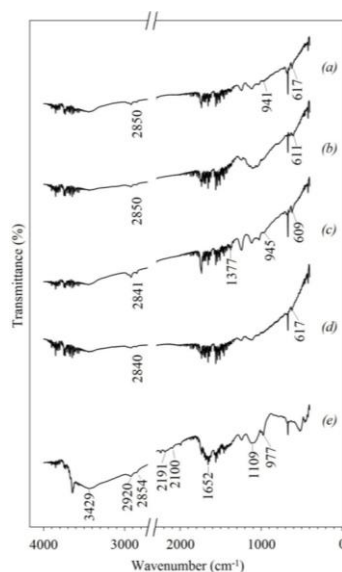


Fig. 6. FTIR spectroscopy results of a- CuS/FNBR obtained in 8 cycles using Na<sub>2</sub>S (25°C air dried), b- CuS/FNBR obtained in 8 cycles using Na<sub>2</sub>S (100°C vacuum dried), c- CuS/FNBR obtained in 8 cycles using thiourea (25°C air dried), d- CuS/FNBR obtained in 8 cycles using thiourea (100 °C vacuum dried), e- FNBR.

#### 4. Conclusions

Using different copper precursors ( $\text{CuSO}_4 \times 5\text{H}_2\text{O}$ ,  $\text{CuCl}_2 \times 2\text{H}_2\text{O}$ ) and sulfur precursors ( $\text{Na}_2\text{S} \times 9\text{H}_2\text{O}$  and thiourea  $[(\text{NH}_2)_2\text{CS}]$ ) copper sulfide nanoparticles were successfully synthesized on the base of functionalized nitrile butadiene rubber (FNBR) at room temperature by the successive ionic layer adsorption and reaction (SILAR) method. From the XRD pattern, no other characteristic peaks corresponding to any impurity was obtained, indicating the purity of the product.

Using  $\text{CuCl}_2 \times 2\text{H}_2\text{O}$  as a copper precursor in different sulfur sources like sodium sulfide and thiourea, phase-pure hexagonal CuS nanocrystals were synthesized. The formation of different crystal phases like  $\text{Cu}_{1.8}\text{S}$  and CuS can be explained as due to the copper precursors.  $\text{CuSO}_4 \times 5\text{H}_2\text{O}$  has an oxidizing nature and by this precursor, the reaction goes by the formation of not II valence copper sulfide. But the reaction with  $\text{CuCl}_2 \times 2\text{H}_2\text{O}$  goes by the formation of pure hexagonal covellite CuS. In this way, the synthesis of II valence copper sulfide can be explained that the ion exchange reaction occurred in the process.

The average particle size of CuS and  $\text{Cu}_{1.8}\text{S}$  were in the range of 10-10.8 nm and 5-7 nm by XRD, respectively. The element ratio of Cu:S was found to be 4:3.8 and 2:1 for CuS and  $\text{Cu}_{1.8}\text{S}$  nanoparticles.

#### References

- [1] D.F.A.Koch, M.J.Mcintyre, J. Electroanal. Chem. **71**, 285 (1976)
- [2] M.C.Lin, M.W.Lee, Electrochemistry Communications. **13**, 1376 (2011)
- [3] L.Gao, E.Wang, S.Lian, Z.Kang, Y.Lan, D.Wu, Solid State Communications. **130**, 309 (2004)
- [4] Q.Y.Lu, F.Gao, D.Y.Zhao, Nano Lett. **2**,725 (2002)
- [5] P.Roy, K.Mondal, S.Kumar Srivastava, Crystal Growth and Design. **8**, 1530 (2008)
- [6] P.Roy, S.K.Srivasta, Mater. Lett. **61**, 1693 (2007)
- [7] X.Jiang, Y.Xie, J.Lu, W.He, L.Zhu, Y.Qian, J. Mater. Chem. **10**, 2193 (2000)
- [8] M.Saranya, A.N.Grace, Journal of Nano Research **18-19**, 43 (2012)
- [9] H.Xu, W.Wang, W.Zhu, Materials Letters. **60**, 2203 (2006)
- [10] H.Zhang, Y.Zhang, J.Yu, D.Yang, Journal of Physical Chemistry C. **112**, 13390 (2008)
- [11] J.Zhang, J.Yu, Y.Zhang, Q.Li, J.R.Gong, Nano Lett. **11**, 4774 (2011)
- [12] Y.Zhu, X.Guo, J.Jin, Y.Shen, X.Guo, W.Ding, J Mater Sci. **42**, 1042 (2007)
- [13] L.Xua, X.Chena, L.Mab, F.Gao, Colloids Surf. A. **349**, 69 (2009)
- [14] L.Zhao, F.Tao, Z.Quan, X.Zhou, Y.Yuan, J.Hu, Materials Letters. **68**, 28 (2012).
- [15] J.Yu, J.Zhang, Sh.Liu. J. Phys. Chem. C, **114**, 13642 (2010).
- [16] Y.Wang, Y.Hu, Q.Zhang, J.Ge, Z.Lu, Y.Hou, Y.Yin, Inorganic Chemistry. **49**, 6601 (2010)
- [17] S.Jiao, L.Xu, K.Jiang, D.Xu, Adv. Mater. **18**, 1174 (2006)
- [18] A.Astam, Y.Akaltun, M.Yildirim, Turk J Phys. **38**, 245 (2014)
- [19] Z.Wu, Ch.Pan, Z.Yao, Q.Zhao, Y.Xie, Cryst. Growth Des. **6**, 1414, (2006)
- [20] Z.Li, H.Yang, Y.Ding, Y.J.Xiong, Y.Xie. Dalton Trans. **1**, 149 (2006)
- [21] X.L.Yu, C.B.Cao, H.S.Zhu, Q.S.Li, C.L.Liu, Q.H.Gong, Advanced Functional Materials. **17**, 1397 (2007)
- [22] P.V.Q.Ramirez, M.C.A.Arrocena, J.S.Cruz, M.V.González, et al., Beilstein J. Nanotechnol. **5**, 1542 (2014)
- [23] G.Y.Chen, B.Deng, G.B.Cai, W.F.Dong, W.X.Zhang, A.W.Xu, Crystal grows and design. **8**, 2137 (2008)
- [24] M.T.S.Nair, L.Guerrero, P.K.Nair, Semicond. Sci. Technol. **13**, 1164 (1998)
- [25] L.Reijnen, B.Meester, A.Goossens, et al., J. Chem. Vap. Deposition. **9**, 15 (2003).
- [26] C.Nascu, I. Pop, V.Ionescu, E.Indrea, I.Bratu, J. Mater. Lett. **32**, 73 (1997)
- [27] O.O.Balayeva, A.A.Azizov, N.O.Balayeva, R.M.Alosmanov, Molodoy Ucheniy. **40**, 118 (2012)
- [28] N.O.Balayeva, O.O.Balayeva, A.A.Azizov, R.M.Alosmanov, G.M.Eyvazova, M.B.Muradov, J. Composites: Part B. **53**, 391 (2013)

- [29] O. O. Balayeva, A. A. Azizov, M. B. Muradov, A. M. Maharramov, G. M. Eyvazova, R. M. Alosmanov, Z. Q. Mamiyev, Z. A. Aghamaliyev, *Materials Research Bulletin*. **75**, 155 (2016)
- [30] J. Kundu, D. Pradhan. *New J. Chem.* **37**, 1470 (2013)
- [31] S. Janaa, N. Mukherjeeb, B. Chakrabortyc, B. C. Mitrad, A. Mondal, *Applied Surface Science*. **300**, 154 (2014)
- [32] W. Li, A. Shavel, R. Guzman, J. R. Garcia, C. Flox, J. Fan, D. Cadavid, M. Ibanez et al. *Chem. Commun.* **47**, 10332 (2011)
- [33] M. B. Muradov, G. M. Eyvazova, E. Y. Malikov, O. O. Balayeva, *International Journal of Innovative Science, Engineering & Technology*. **1**, 352 (2014)
- [34] N. O. Balayeva, Z. Q. Mamiyev, *Materials Letters*. **162**, 121 (2016)
- [35] S. G. Dixit, A. R. Mahadeshwar, S. K. Haram. *Colloids Surf. A: Physicochem. Eng. Aspects*. **133**, 69 (1998)